RSC Advances

PAPER

View Article Online
View Journal | View Issue

Cite this: *RSC Adv.*, 2017, **7**, 52684

Preparation and properties of lambda-cyhalothrin/polyurethane drug-loaded nanoemulsions

He Qin,† Hong Zhang,† Lingxiao Li, Xiaoteng Zhou, Junpei Li and Chengyou Kan *

Conventional pesticide formulations are usually used inefficiently due to loss and poor foliage adhesion, which results in a large waste of resources and serious environmental pollution. In order to prolong the foliar pesticide retention and release time, using biodegradable castor-oil based polyurethane (CO-PU) as a carrier, lambda-cyhalothrin/CO-PU (LC/CO-PU) nanoemulsions were prepared *via* an *in situ* soap-free phase inverse emulsification technique and their properties were investigated. Results showed that the LC/CO-PU nanoemulsions had a good water dispersion and the drug-loaded nanoparticles (NPs) were uniform spheres with diameters of less than 80 nm. The LC physically encapsulated in the CO-PU carrier was in an amorphous state, and the maximum of the LC loading capacity was around 40 wt% with a high encapsulation efficiency of more than 85%. Compared with commercial LC formulations, the LC/CO-PU nanoemulsions exhibited a sustained and controlled-release property, which could be adjusted by the LC loading capacity and temperature. The foliage adhesion of the LC/CO-PU nanoemulsions was much better than that of the commercial LC formulations due to the low surface tension, larger chain mobility of the LC/CO-PU systems as well as hydrogen-bond interactions between the polyurethane and foliar surface, which was of great significance to achieve the efficient use of pesticides.

Received 26th September 2017
Accepted 9th November 2017

DOI: 10.1039/c7ra10640h

rsc.li/rsc-advances

Introduction

As very important agrochemicals, pesticides have been widely used to control pests, protect crops and increase the yield of crops. However, depending on the application methods and climate conditions, only a small amount of the pesticide can stay on the foliage[1–3] and only about 0.1% can finally affect the pests.[4,5] At present, the commonly used commercial pesticide formulations are emulsifiable concentrates (EC) and wettable powders (WP), which usually lead to a waste of resources and serious environmental pollution owing to the large dose of dispersing agent or organic solvent.[6,7] In order to solve the problems of pesticide waste and environment pollution, more and more attention has been paid to developing efficient and green pesticide formulations.

Pesticide-loaded systems, which combine the pesticide with a suitable carrier, are a feasible method to overcome the drawbacks of conventional pesticide formulations.[8–10] An appropriate carrier can significantly improve the adhesion of pesticide on the foliage surface so as to prolong residence time and reduce the loss of the pesticide,[11,12] and also make continuous and stable release of the pesticide possible.[13–15] With the development of nanotechnology, pesticide-loaded nano-system shows a great potential to be applied in the field of pesticide loading due to its good foliage deposition and high permeability to pests.[16,17]

Lambda-cyhalothrin (LC), recognized as a high-efficient bionic pesticide with a broad insecticidal spectrum, has been widely used in different crops such as cotton and corn. However, commercial LC formulations have the same drawbacks of large dose of additives, pesticide loss and environment pollution due to its poor water solubility.[6,16] Thus, some materials such as SiO_2,[18] alginate derivatives,[19,20] polylactic acid[4] and copolymer[21] have been used as carriers to develop the LC-loaded systems in recent years. Although these LC-loaded systems showed certain stability and controlled-release property, most of them were prepared by relative complex techniques and the size of drug-loaded particles were over 100 nm, which did not conform to the requirement of nanotechnology.[22] Besides, few research have paid attention to the interaction between pesticide and foliage surface, which is a significant criterion to evaluate the adhesion performance of LC. Thus, a simple and efficient method to prepare LC-loaded nano-system with good foliage adhesion is desirable.

Polyurethane (PU), a kind of synthetic polymer material with good structure controllability and biocompatibility, has been applied in medical devices[23,24] and drug delivery systems.[25,26] Currently, the low-toxic and biodegradable castor oil-based PU (CO-PU) has been prepared by using renewable castor oil as raw

Department of Chemical Engineering, Key Laboratory of Advanced Materials of Ministry of Education of China, Tsinghua University, Beijing 100084, China. E-mail: kancy@mail.tsinghua.edu.cn

† These authors contributed equally to this work.

material.[27,28] On the other hand, the self-emulsifying technique has been used to fabricate PU emulsion in the absence of the emulsifier,[29] which no longer needs extra surfactants in the PU emulsion preparation so as to reduce production costs and pollution. However, few research have concentrated on PU-containing pesticide-loaded systems, especially for the nano-systems.[30,31]

In this work, LC/CO-PU nanoemulsions were first prepared by *in situ* soap-free phase inverse emulsification, and the chemical composition, the colloidal and drug-loaded properties, the drug controlled release behavior as well as the adhesive property on different crop foliage were investigated, and a mechanism of enhancing foliage adhesion was proposed.

Experimental section

Materials

Lambda-cyhalothrin (96%) was supplied by the Chinese Academy of Agriculture Science. Isophorone diisocyanate (IPDI), polyether diol (N_{220}, M_n = 2000) and dimethylolpropionic acid (DMPA) were purchased from Beijing Linshi Chem Co. Ltd, China. Castor oil (CO) was purchased from Nanjing Weier Chem Co. Ltd, China. Dibutyltin dilaurate (DBTDL) was purchased from Tianjin Guangfu Fine Chemical Research Institute, China. 1,4-Butanediol (BDO) was purchased from Tianjing bodi Chem Co. Ltd, China. Triethylamine (TEA), acetone, ethanol and cyclohexane were purchased from Beijing chemworks, China. The emulsifiable concentrare formulation of LC (LC-EC, 2.5 wt%) was purchased from Beijing Zhongbao Agriculture Co. Ltd, China. The wettable powder formulation of LC (LC-WP, 10 wt%) was purchased from Jiangsu Yangnong Chemical Group Co. Ltd. Deionized water was used throughout.

Preparation of LC/CO-PU nanoemulsions

LC/CO-PU nanoemulsions were prepared by *in situ* soap-free phase inverse emulsification process. 3.67 g of IPDI, 4.00 g of N_{220}, 1.38 g of CO and 2 drops of DBTDL were first charged into a 100 mL three-necked round-bottom flask equipped with an electric mechanical stirrer and a reflux condenser, and the mixture was heated to 80 °C with the stirring speed of 300 rpm. After 2 h of reaction, 0.54 g of DMPA dissolved in 1 mL of acetone was added into the flask to perform the chain extension for 1 h, and then the solution of BDO (0.27 g) in acetone (1 mL) was added and the chain-extension reaction continued for another 2 h. After then, the reaction system was cooled to room temperature and the mixture of 0.41 g TEA and 2 mL acetone was charged into the system. After 0.5 h of neutralization, the CO-PU prepolymer was prepared.[32]

Subsequently, according to the designed formula in Table 1, certain amount of the pre-dissolved LC solution in acetone and the CO-PU prepolymer was first mixed, and a predetermined amount of water was then charged into the system, and *in situ* soap-free phase inversion emulsification was conducted at 1100 rpm for 40 min. Finally, the LC/CO-PU nanoemulsions were obtained by removing acetone with vacuum rotary evaporation.

Characterization of the LC/CO-PU nanoemulsions

Chemical composition. The ingredients of the LC/CO-PU systems were qualitatively determined *via* a Fourier transform infrared spectrometer (FTIR, Nicolet 560; Thermo Fisher Scientific, USA). The free LC solid powder in KBr and the latex films formed by drying the nanoemulsions at room temperature were used to do measurement.

Colloidal property. The hydrodynamic diameter (D_p), polydispersity index (PI), and zeta potential (ζ) of the LC/CO-PU NPs were measured with laser scatter method (Zetasizer 3000 HS; Malvern, UK) at 25 °C. The morphology of the dried NPs was observed on a transmission electron microscope (TEM, H-7650B; Hitachi, Japan) with an accelerating voltage of 80 kV, and the samples were obtained by spreading and drying the diluted nanoemulsions (nanoemulsion/water, 1 : 200, v/v) on carbon-coated copper grids with phosphotungstic acid as stain agent.

Thermal property. The thermal behavior of the free LC solid powder, CO-PU and LC/CO-PU latex films were examined by a differential scanning calorimeter (DSC, Q5000IR; TA Instruments, USA). About 5 mg of the sample was weighted accurately and first heated from 20 °C to 120 °C at 20 °C min^{-1} and held at 120 °C for 10 min to eliminate thermal history. Then, the sample was cooled to −90 °C at 20 °C min^{-1} and after an isothermal process for 3 min, it was heated to 120 °C at 10 °C min^{-1}.[33] The glass transition temperature (T_g) and the melt point (T_m) were obtained from the DSC curve.

Solid content. The solid content (ω) of the LC/CO-PU nanoemulsion was determined thermogravimetrically. About 1 g of the nanoemulsion (W_2) was weighted accurately and put into a pre-weighed bottle (W_1), and the bottle was then placed in an oven at 80 °C. 24 h later, the bottle was taken out from the oven and weighted again (W_3). The solid content of the nanoemulsion was calculated according to eqn (1).

Table 1 Formula of the LC/CO-PU nanoemulsions

Sample	Designed drug loading capacity (wt%)	Designed solid content (wt%)	LC (g)	Acetone (mL)	H_2O (g)
S1	10	30	1.19	1.0	26.72
S2	20	30	2.67	2.0	30.17
S3	30	30	4.58	3.0	34.63
S4	40	30	7.13	4.0	40.58

$$\omega\ (\mathrm{wt\%}) = \frac{W_3 - W_1}{W_2} \times 100\% \quad (1)$$

Drug loading capacity. The drug loading capacity (DL) is defined as the mass percentage of the loaded LC to the total solid in the LC/CO-PU nanoemulsion. The resulted LC/CO-PU nanoemulsion was first placed at 25 °C for 24 h, and centrifuged with a speed of 10 000 rpm. Then, the supernatant was dried at room temperature to form latex films. About 20 mg of the latex film was weighted accurately and immersed into 10 mL of cyclohexane, and the mixture was kept under the ultrasound for 1 h to make LC release completely. The mass concentration of LC in cyclohexane was examined by UV-vis spectrophotometer (T6; Pgeneral, China) under a detection wavelength of 278 nm, and the drug loading capacity of the nanoemulsion was calculated according to eqn (2).

$$\mathrm{DL}\ (\mathrm{wt\%}) = \frac{c \times V}{m} \times 100\% \quad (2)$$

where c is the mass concentration of LC in cyclohexane, V is the volume of the cyclohexane, and m is the mass of the latex film.

Encapsulation efficiency. The encapsulation efficiency (EE), defined as the mass percentage of the loaded LC calculated from mass of nanoemulsion (M_1) to the total LC (M_2) used in the preparation recipe, was calculated according to eqn (3).

$$\mathrm{EE}\ (\%) = \frac{M_1 \times \omega \times \mathrm{DL}}{M_2} \times 100\% \quad (3)$$

Surface tension. The surface tension of the diluted nanoemulsion with drug content of 1 g L^{-1} was directly tested on a surface tension meter (DCAT21; Dataphysics, Germany) at 25 °C. The surface tension of CO-PU latex film was calculated by Antonow equation[34] and Lifshitz-vander waals acid–bases (LW-AB) approach[35,36] using the contact angles of water, glycerol and ethylene glycol on the CO-PU latex film, in which the contact angles were measured by a contact angle meter (JC2000C1; Powereach, China) at 25 °C.

Controlled-release behavior of the LC/CO-PU nanoemulsions. The release behaviors of the LC/CO-PU nanoemulsions and the commercial LC formulations were evaluated as follows. Each sample containing 10 mg of LC was first suspended in 10 mL of ethanol/water mixture (1 : 1, v/v) and charged into a dialysis bag, and the bag was then immersed into 100 mL of ethanol/water mixture (1 : 1, v/v) in a wide-mouth flask. After then, the flask was placed in a shaking incubator (HZ-9210K; Hualida, China) at pre-set temperatures with a shaking speed of 150 rpm. During dialyzing, 3 mL of the dialysis solution outside the dialysis bag was collected at specified time intervals, and at the same time, 3 mL of fresh ethanol/water mixture was supplemented into the flask. The LC concentration of the solution was measured by UV-vis spectroscopy at a wavelength of 278 nm, and the accumulated release rate of LC for each sample was calculated by the concentrations of LC dissolved in release medium at different times.

Foliage adhesion of the LC/CO-PU nanoemulsions. The cotton and corn leaves were used to assess the adhesion behavior of the LC/CO-PU nanoemulsions, and the sample S3 was chosen because of its high drug content and long-time stability. The LC formulations with LC content of 1 g L^{-1} in water were first sprayed onto the fresh and washed cotton and corn leaves, and after naturally dried in air, each of the samples was divided into two parts. One part was continuously washing with running water for 0.5 h, and the other part was not treated. After dried in air for 1 h and followed by gold-spraying treatment, the surface morphology of the sample was characterized on a scanning electron microscope (SEM, Vaga3; Tescan, Czech) with an accelerating voltage of 20 kV.

Results and discussion

Preparation of LC/CO-PU nanoemulsions

A facile and economic method was used to fabricate LC/CO-PU nanoemulsions, in which the CO-PU prepolymer with hydrophilic carboxyl groups was first synthesized by step-growth addition polymerization (Fig. 1),[32] and then the homogeneous acetone solution of the CO-PU prepolymer and LC was dispersed in water through vigorous stirring *via* self-emulsification process as shown in Fig. 2. Since LC was water-insoluble, during the *in situ* phase inversion process, the LC molecules tended to enter into the CO-PU NPs to form stable LC/CO-PU nanoemulsions.

Compared with conventional petroleum-based PU, the introduction of CO in PU molecular chain not only saved the cost, but also made the PU carrier biodegradable.[27,28] Moreover, since the average hydroxyl functionality of CO was 2.7, the cross-linking reaction of CO made the CO-PU carrier to form a network structure as shown in Fig. 2, which was beneficial to trap LC and improve the thermal stability and UV resistance of the CO-PU carrier.[27]

Composition and structure of the LC/CO-PU nanoemulsions

The composition of LC/CO-PU drug-loaded systems was investigated by FTIR analysis. In the spectrum of CO-PU (Fig. 3a), the peak at 3323 cm^{-1} was due to the stretching vibration of –NH– in urethane or urea groups, of which the –CO– stretching vibration was split into peaks at 1695 and 1531 cm^{-1}. For the spectrum of free LC (Fig. 3f), the stretching vibration of benzene skeleton was at 1586 and 1492 cm^{-1}, and the carbonyl stretching vibration of ester group appeared at 1722 cm^{-1}. Obviously, the characteristic peaks of both the CO-PU carrier and free LC appeared in the spectrum of LC/CO-PU drug-loaded system (Fig. 3b–e) without any new peaks, indicating that the pesticide LC was physically loaded in CO-PU carrier and the chemical properties of LC were not changed.[37]

As the DSC curves in Fig. 4 indicated, the free LC solid powder had a T_m at 51.4 °C, while there was no any peak around this temperature in the LC/PU systems (Fig. 4a), demonstrating that the state of LC loaded in the LC/PU systems was changed from crystal to amorphous, which was

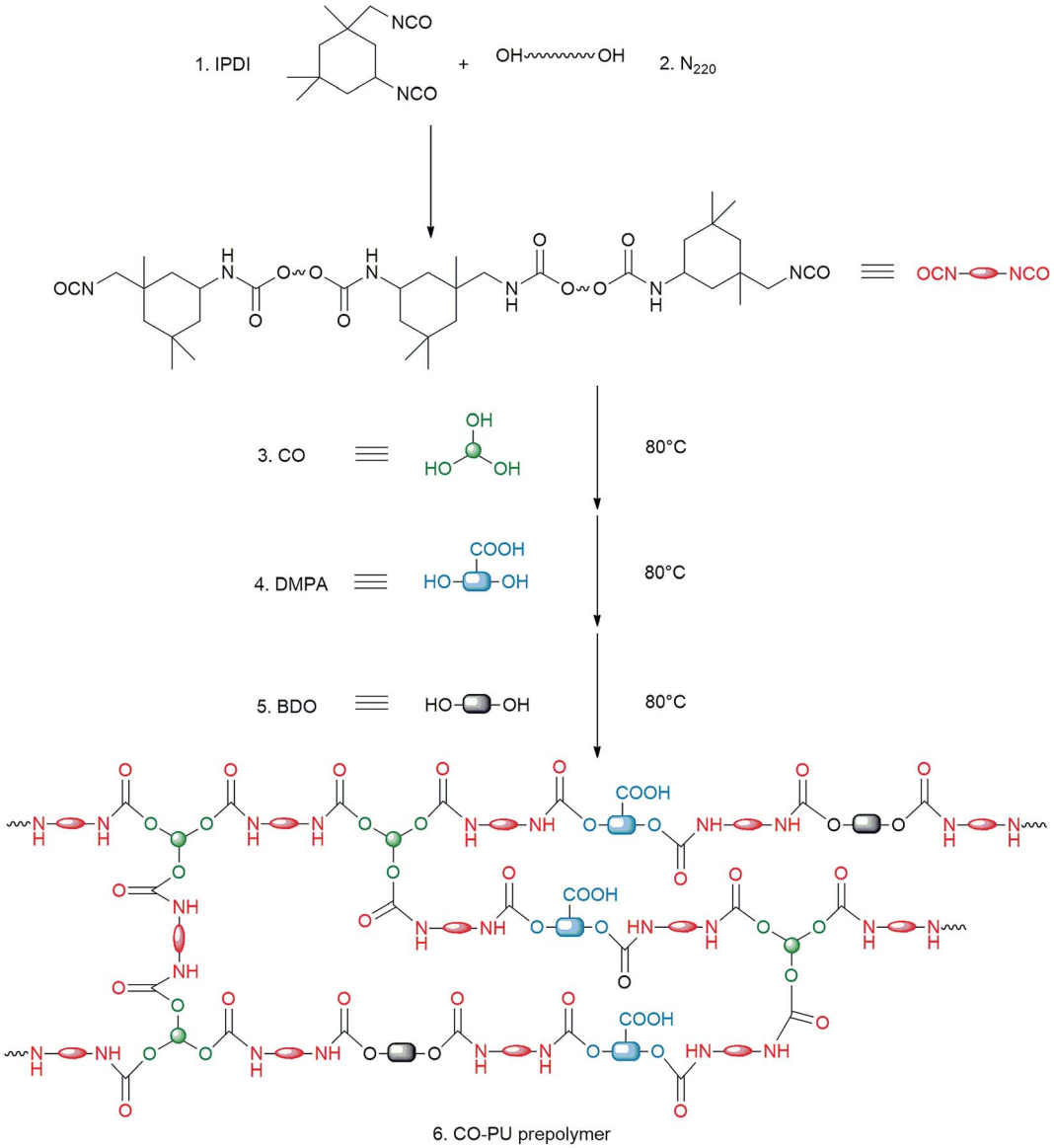

Fig. 1 Synthesis route of the CO-PU prepolymer.

beneficial to improve solubility and bioavailability of the pesticides.[38]

It was worth noting that, the T_g of CO-PU in the drug-loaded systems increased with the increase of LC loading capacity (Fig. 4b). This phenomenon might result from the formation of hydrogen bond or other interactions between the F atoms of LC and the active H atoms of CO-PU carrier, which contributed to the forming of an extra physical crosslinking[39] in drug-loaded systems and the increase of T_g.

Colloidal properties of the LC/CO-PU nanoemulsions

The dispersion capacity and stability of pesticide aqueous formulations are vital for their storage and application in practice. As listed in Table 2, the hydrodynamic size (D_p) of the LC/CO-PU nanoemulsions with a narrow size distribution (PI) increased with the increase of LC loading capacity, which was in accord with the TEM observation results (Fig. 5). The nanoscale and uniform spherical morphology of the LC/CO-PU nanemulsions were favorable to the improvement of the adhesion on crop foliage and permeability to the pests of the nanoemulsions.[16]

The storage stability of the nanoemulsions was also tested at room temperature. As shown in Fig. 6, after a three-month storage, the nanoemulsions with the designed LC loading capacity less than 30 wt% (sample S1–S3) were still stable and homogeneous without any deposition. However, when the designed LC loading capacity increased to 40 wt% (sample S4), a little amount of LC precipitation was observed in the nanoemulsion, indicating the increase of water-insoluble LC content would decrease the stability of the nanoemulsions, which was also consistent with the value of ζ in Table 2.

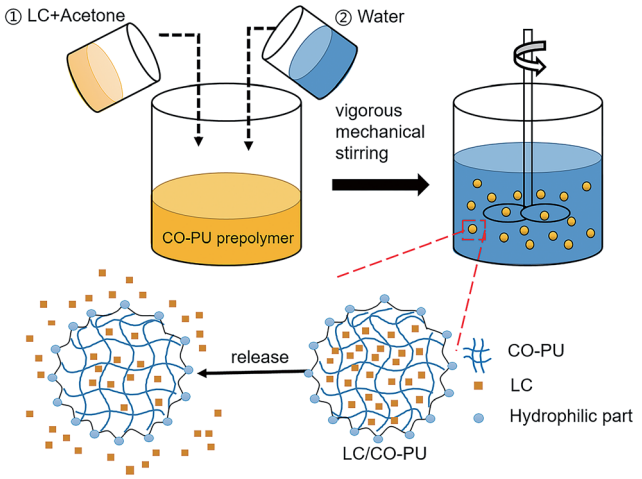

Fig. 2 Schematic diagram of the preparation and release of the LC/CO-PU nanoemulsion.

Thus, sample 4 was excluded in the release behavior investigation.

Drug loading capacity and encapsulation efficiency of the LC/CO-PU nanoemulsions

Drug loading capacity and encapsulation efficiency are both important properties for drug-loaded systems. As indicated in Table 3, the measured solid content (ω) and drug loading capacity (DL) of the LC/CO-PU nanoemulsions were close to their designed value in Table 1, and encapsulation efficiency (EE) was more than 85%, demonstrating that most of LC was loaded into the CO-PU carrier.

Release behavior of the LC/CO-PU nanoemulsions

The release behaviors of LC from the LC/CO-PU nanoemulsions with different LC loading capacities were investigated in ethanol/water mixture (1 : 1, v/v) at different temperatures.

Fig. 7 presented the release profiles of the LC-loaded nanoemulsions, the commercial LC-EC and LC-WP formulations at 25 °C. Apparently, LC-EC and LC-WP released very fast at an early stage and reached equilibrium after 48 h, and the accumulated releases were over 90%. However, the release rate of all the LC/CO-PU nanoemulsions was rapid just within the first 30 h, then it slowed down and maintained a stable release

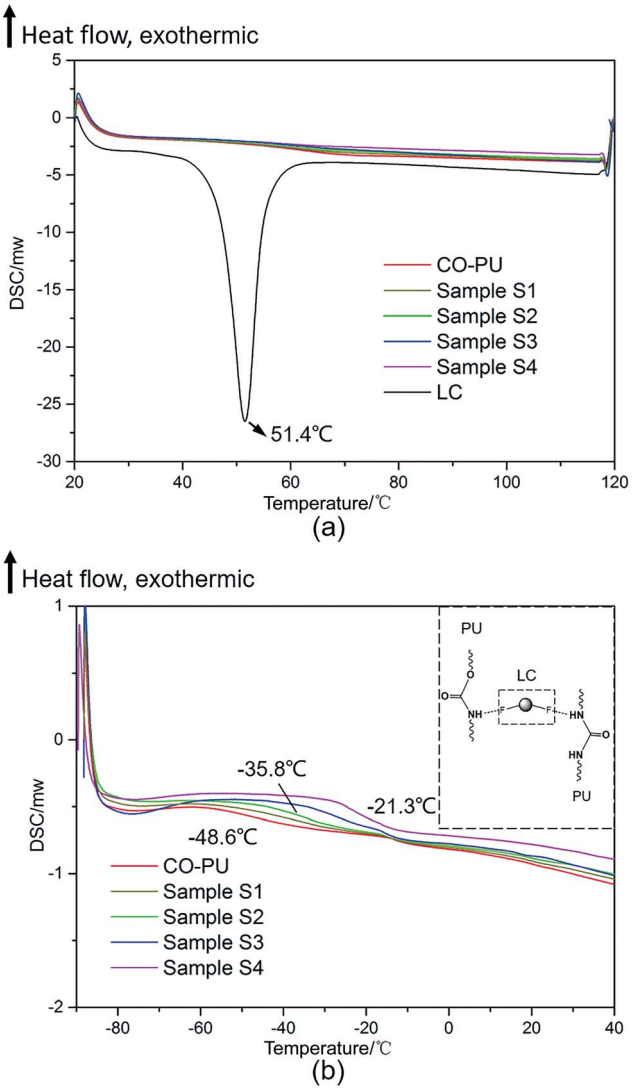

Fig. 4 DSC curves of the CO-PU, the free LC and the LC/CO-PU systems.

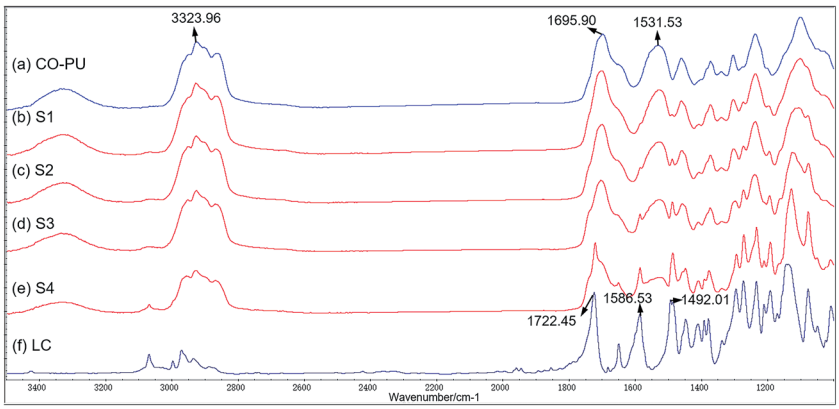

Fig. 3 FTIR spectra of the CO-PU carrier (a), the LC/CO-PU systems sample S1–S4 (b–e) and the free LC (f).

Table 2 Colloidal properties of the LC/CO-PU nanoemulsions

Sample	D_p (nm)	PI	ζ (mV)
S1	42.3 ± 1.4	0.112 ± 0.01	−59.8 ± 1.7
S2	49.6 ± 1.7	0.109 ± 0.01	−57.3 ± 1.2
S3	69.7 ± 1.3	0.112 ± 0.01	−54.3 ± 2.4
S4	75.5 ± 0.9	0.0806 ± 0.02	−51.5 ± 2.9

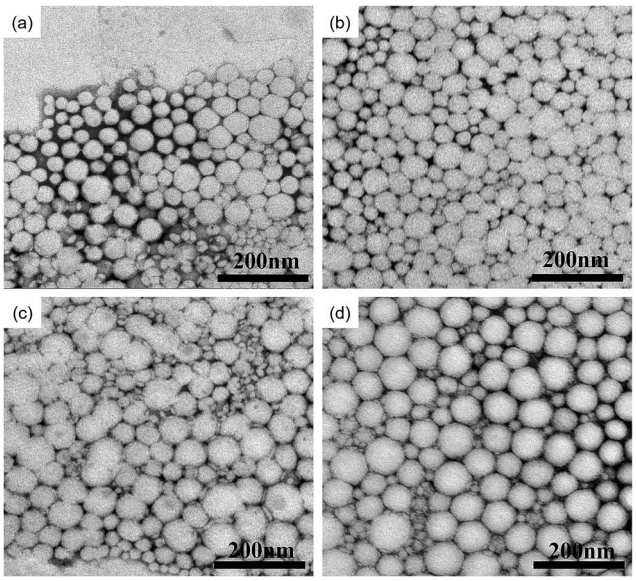

Fig. 5 TEM images of the LC/CO-PU nanoparticles: (a) S1; (b) S2; (c) S3; (d) S4.

until equilibrium after 80 h. Compared with the commercial formulations, the LC/CO-PU nanoemulsions exhibited a slower release rate and a longer sustained release period. It should be pointed out that the release profiles measured in ethanol/water medium did not represent the practical release behavior in actual agricultural environment, and the release rate of the LC/CO-PU systems would be much slower in actual utilization.[4]

Effect of the drug loading capacity on the release behavior

As shown in Fig. 7, the accumulated release of LC from the LC/CO-PU nanoemulsions increased from 65.6% to 71.9% after 72 h with the increase of drug loading capacity from 10 wt% to

Table 3 Solid content, drug loading capacity and encapsulation efficiency of the LC/CO-PU nanoemulsions

Sample	ω (wt%)	DL (wt%)	EE (%)
S1	29.60	10.62 ± 0.46	93.75 ± 2.80
S2	29.57	20.91 ± 1.08	89.09 ± 4.35
S3	29.04	29.73 ± 1.50	85.61 ± 4.31
S4	28.53	39.28 ± 1.69	85.54 ± 3.22

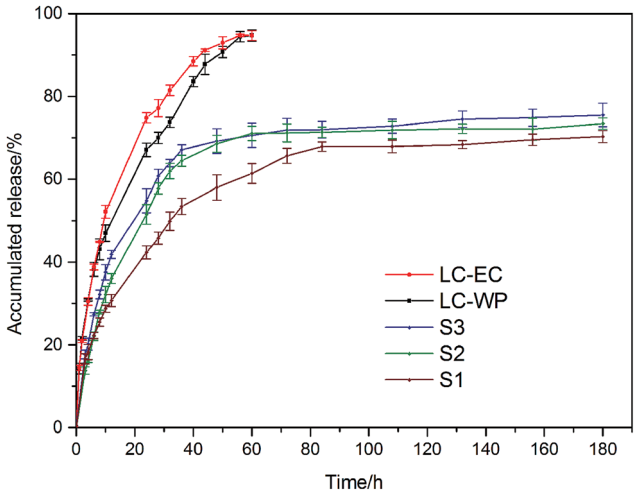

Fig. 7 Release profiles of the LC-EC, LC-WP and LC/CO-PU nanoemulsions with different LC loading capacities at 25 °C.

30 wt%. A higher LC-loading capacity in the LC/CO-PU nanoemulsions provided the NPs with a greater concentration gradient of LC between internal and external environment, which made the pesticide molecules dissolve and migrate to the surrounding more easily, resulting in a faster release. Besides, a higher LC loading capacity in the NPs would lead to the form of the looser network structure of CO-PU carrier, which also accelerated the release.

Effect of temperature on the release behavior

The LC release of the sample S3 was investigated at different temperatures. As shown in Fig. 8, the release rate at different temperatures also followed "fast then slow" trend, and the

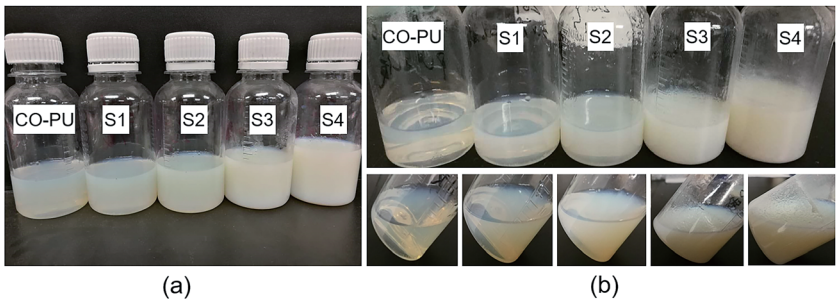

Fig. 6 Optical photos of the nanoemulsions (from left: CO-PU, S1, S2, S3, and S4): before (a) and after (b) three-month storage.

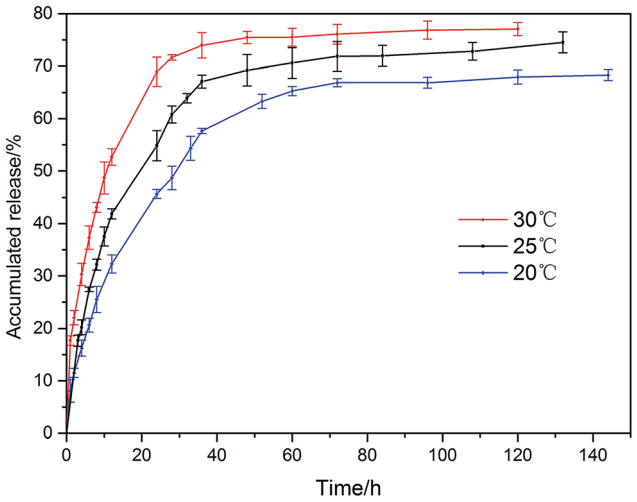

Fig. 8 Release profiles of the LC/CO-PU nanoemulsion (sample S3) at different temperatures.

accumulated release increased from 66.9% to 76.1% after 72 h as the temperature rose from 20 °C to 30 °C. As the diffusion of the LC molecules were accelerated at a higher temperature, the pesticides had an easier and faster release from the LC/CO-PU nanoemulsion.

Release mechanism of the LC/CO-PU nanoemulsions

In order to investigate the release mechanism of the LC/CO-PU nanoemulsions, the simple exponential relation (4) on drug delivery proposed by Ritger and Peppas was applied to analyze the release profiles:[40]

$$\frac{M_t}{M_\infty} = kt^n \quad (4)$$

where M_t is the accumulated release of LC at time t, M_∞ is the accumulated release of LC as time approaches infinity, k is a constant and n is the diffusional exponent. The correlation coefficient R^2, diffusional exponent n and T_{50} (the time required for the drug quantity to release to 50% of its initial value) were calculated and listed in Table 4. Due to the correlation coefficients R^2 were over 0.97, there was a good correlation between the LC release profiles and Ritger–Peppas equation. The decrease of T_{50} from sample S1 to sample S3 also indicated that the nanoemulsions with high drug loading capacity could achieved a faster release. Moreover, the diffusional exponent n was larger than 0.43, indicating that the LC release from the LC/CO-PU nanoemulsions belonged to non-Fickian transport, and the release was triggered by the NPs swelling and the LC molecule diffusing.

Table 4 Parameters of fitting the Ritger–Peppas equation to the release profiles of the different LC/CO-PU nanoemulsions

Sample	R^2	n	T_{50} (h)
S1	0.9943	0.4364	36.23
S2	0.9730	0.4960	24.64
S3	0.9876	0.4705	20.15

Foliage adhesion of the LC/CO-PU nanoemulsions

A high foliage adhesion is always desired for the pesticide-loaded systems, which can increase the retention of pesticides on crop surfaces and decrease the loss. To prove that the LC/CO-PU nanoemulsions have a better adhesion property on crop surfaces than other commercial LC formulations, the adhesion experiments were conducted,[41] and results were displayed in Fig. 9. As indicated, the similar LC deposited situations were observed for the three LC formulations on both the cotton and corn foliar surfaces without washing (Fig. 9a–c and e–g). After being washed with water, most of particles still remained on the leaves for the LC/CO-PU nanoemulsion (Fig. 9a′ and e′), while only a few of particles adhered on the leaves for both commercial LC-EC and LC-WP formulations (Fig. 9b′, c′, f′ and g′). These results clearly indicated that the LC/CO-PU nanoemulsions had stronger adhesion on crop leaves than the LC-EC and LC-WP formulations.

In order to further understand the adhesion mechanism of the LC/CO-PU nanoemulsions on the foliage, the adhesion processes including spreading, deposition and molecular interaction between nanoemulsion and foliage were considered, as shown in Fig. 10. During the spraying, aqueous droplets of the LC/CO-PU nanoemulsion were spread on the foliage surface firstly (Fig. 10a). Note that, the surface tension of each formulation (γ_l) listed in Table 5 was less than the critical surface tension (γ_c) of cotton and corn leaves listed in Table 6,[42] implying that each formulation could wet on the cotton and corn leaves. Because the surface tension of the LC/CO-PU nanoemulsion was close to that of the LC-EC and LC-WP formulations, the nanoemulsion could achieve a similar wettability to the commercial LC formulations in the case without using a large number of emulsifiers and additives.

Subsequently, the drug-loaded NPs aggregated and coalesced to form latex films on the foliage with the volatilization of water (Fig. 10b). As given in Fig. 4b, the T_g of the LC/CO-PU systems was from −48 °C to −21 °C, and this low T_g would be favorable to the deformation of drug-loaded NPs through the motion of CO-PU molecular chains. In addition, as listed in Table 8, the surface tension of the LC/CO-PU latex film (γ_s), which was calculated by Antonow[33] and LW-AB[34,35] equations using the contact angles of three liquids on the latex film (sample 3) shown in Table 7, was less than the critical surface tension (γ_c) of cotton and corn leaves, meaning that the LC/CO-PU latex film could also spread on the foliage surface. Thus, both the T_g and γ_s were beneficial to form latex films on the cotton and corn leaves which enlarged the contact between nanoparticles and foliage.

Furthermore, there are a great quantity of urethane and urea groups in the CO-PU chains, which are able to form the

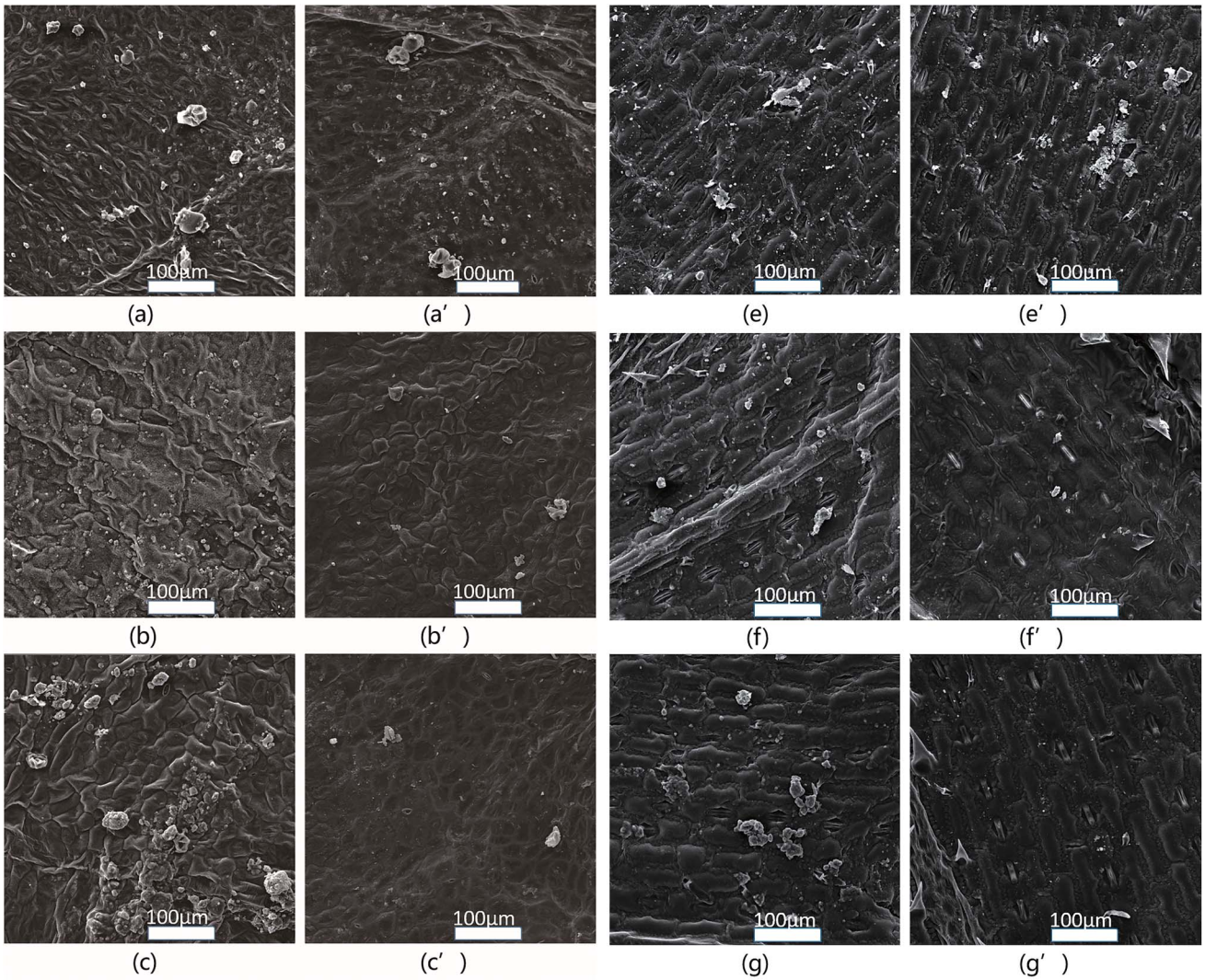

Fig. 9 SEM images of the different LC formulations on the cotton leaves (left) and the corn leaves (right): LC/CO-PU nanoemulsion (sample S3) before (a, e) and after (a′, e′) washing; LC-WP formulation before (b, f) and after (b′, f′) washing; LC-EC formulation before (c, g) and after (c′, g′) washing.

hydrogen bonding[11,36] with the water molecules, hydroxyl, carboxyl and aldehyde groups[43] on the surface of the foliage (Fig. 10c). This hydrogen bonding interaction enhanced the adhesion strength between the LC/CO-PU latex films and foliage surface and promoted a longer pesticide retention.

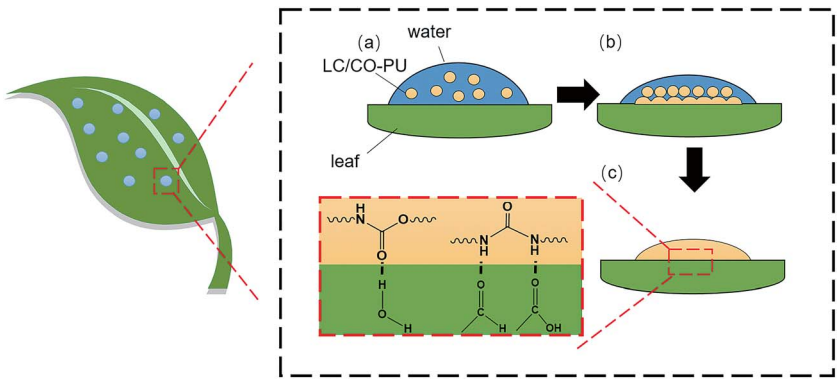

Fig. 10 Adhesion mechanism of the LC/CO-PU nanoemulsions on the crop foliar surface.

Table 5 Surface tension of the different LC formulations

Sample	γ_l (mN m^{-1})
S3	40.32 ± 0.05
LC-WP	34.79 ± 0.03
LC-EC	34.88 ± 0.01

Table 6 Critical surface tension of the cotton and corn leaves

Leaf	γ_c (mN m^{-1})
Cotton	63.30–71.81
Corn	47.40–58.70

Table 7 Contact angles of water, glycerol and ethylene glycol on the latex film (sample S3)

Sample	θ (°)
Water	77.6
Glycerol	66.8
Ethylene glycol	48.1

Table 8 Surface tension of the LC/CO-PU latex film calculated by Antonow and LW-AB methods

	γ_s (mN m^{-1})			
Method	Water	Glycerol	Ethylene	Average γ_s (mN m^{-1})
Antonow	44.22	44.61	40.03	42.95
LW-AB	42.73			42.73

Conclusions

Through a facile and economic method, the LC/CO-PU nanoemulsions with biodegradable CO-PU as the carrier were successfully prepared by *in situ* soap-free phase inverse emulsification technique. The size of LC/CO-PU NPs was less than 80 nm and the LC loading capacity reached as much as 40 wt% with a high encapsulation efficiency more than 85%. The state of the LC physically loaded in the CO-PU NPs was amorphous, which was beneficial to improve the solubility and bioavailability of LC. Compared to the commercial LC-EC and LC-WP formulations, the LC/CO-PU nanoemulsions presented a sustained and long period release of LC, and this release behavior triggered by carrier NPs swelling and the LC molecule diffusion could be accelerated by increasing LC loading capacity and temperature. Moreover, the LC/CO-PU nanoemulsions had a stronger adhesion property on crop leaves than the LC-EC and LC-WP formulations, which benefited from the spreading, deposition and hydrogen bonding interaction between the nanoemulsions and foliage surfaces. As a green and efficient pesticide formulation, the LC/CO-PU nanoemulsions have a great potential to be further explored.

Conflicts of interest

There are no conflicts to declare.

Acknowledgements

This work was financially supported by the National Basic Research Program of China (973 program, no. 2014CB932202).

References

1 M. Song, J. Ju, S. Luo, Y. Han, Z. Dong, Y. Wang, Z. Gu, L. Zhang, R. Hao and L. Jiang, *Sci. Adv.*, 2017, **3**, e1602188.
2 H. N. Guan, D. F. Chi, J. Yu and S. Y. Zhang, *Colloids Surf., B*, 2011, **83**, 148–154.
3 X. Xu, B. Bai, H. Wang and Y. Suo, *ACS Appl. Mater. Interfaces*, 2017, **9**, 6424–6432.
4 B. Liu, Y. Wang, F. Yang, X. Wang, H. Shen, H. Cui and D. Wu, *Colloids Surf., B*, 2016, **144**, 38–45.
5 M. Massinon, N. De Cock, W. A. Forster, J. J. Nairn, S. W. McCue, J. A. Zabkiewicz and F. Lebeau, *Crop Prot.*, 2017, **99**, 65–75.
6 S. N. M. Yusoff, A. Kamari and N. F. A. Aljafree, *Int. J. Environ. Sci. Technol.*, 2016, **13**, 2977–2994.
7 M. C. García, M. C. Alfaro, N. Calero and J. Muñoz, *Carbohydr. Polym.*, 2014, **105**, 177–183.
8 Z. Z. Li, J. F. Chen, F. Liu, A. Q. Liu, Q. Wang, H. Y. Sun and L. X. Wen, *Pest Manage. Sci.*, 2007, **63**, 241–246.
9 F. J. Garrido-Herrera, I. Daza-Fernández, E. González-Pradas and M. Fernández-Pérez, *J. Hazard. Mater.*, 2009, **168**, 220–225.
10 C. Sun, K. Shu, W. Wang, Z. Ye, T. Liu, Y. Gao, H. Zheng, G. He and Y. Yin, *Int. J. Pharm.*, 2014, **463**, 108–114.
11 M. Yu, J. Yao, J. Liang, Z. Zeng, B. Cui, X. Zhao, C. Sun, Y. Wang, G. Liu and H. Cui, *RSC Adv.*, 2017, **7**, 11271–11280.
12 V. Bergeron, D. Bonn, J. Y. Martin and L. Vovelle, *Nature*, 2000, **405**, 772–775.
13 A. Roy, S. K. Singh, J. Bajpai and A. K. Bajpai, *Cent. Eur. J. Chem.*, 2014, **12**, 453–469.
14 T. Fan, J. Feng, C. Ma, C. Yu, J. Li and X. Wu, *J. Porous Mater.*, 2013, **21**, 113–119.
15 W. Sheng, W. Li, G. Zhang, Y. Tong, Z. Liu and X. Jia, *New J. Chem.*, 2015, **39**, 2752–2757.
16 X. Zhao, H. Cui, Y. Wang, C. Sun, B. Cui and Z. Zeng, *J. Agric. Food Chem.*, 2017, DOI: 10.1021/acs.jafc.7b02004.
17 V. Ghormade, M. V. Deshpande and K. M. Paknikar, *Biotechnol. Adv.*, 2011, **29**, 792–803.
18 Y. Xu, W. Chen, X. Guo, Y. Tong, T. Fan, H. Gao and X. Wu, *RSC Adv.*, 2015, **5**, 52866–52873.
19 X. Chen, H. Yan, W. Sun, Y. Feng, J. Li, Q. Lin, Z. Shi and X. Wang, *Polym. Bull.*, 2015, **72**, 3097–3117.
20 J. S. Yang, H. B. Ren and Y. J. Xie, *Biomacromolecules*, 2011, **12**, 2982–2987.
21 T. Fan, X. Wu and Y. Wu, *J. Appl. Polym. Sci.*, 2013, **129**, 1861–1867.
22 B. S. Sekhon, *Nanotechnol., Sci. Appl.*, 2014, **7**, 31–53.
23 A. Lendlein and R. Langer, *Science*, 2002, **296**, 1673–1676.

24 J. P. Santerre, K. Woodhouse, G. Laroche and R. S. Labow, *Biomaterials*, 2005, **26**, 7457–7470.
25 X. Sun, H. Gao, G. Wu, Y. Wang, Y. Fan and J. Ma, *Int. J. Pharm.*, 2011, **412**, 52–58.
26 S. Yu, C. He, J. Ding, Y. Cheng, W. Song, X. Zhuang and X. Chen, *Soft Matter*, 2013, **9**, 2637–2645.
27 R. Bayan and N. Karak, *Polym. Int.*, 2017, **66**, 839–850.
28 H. Yeganeh and P. Hojati-Talemi, *Polym. Degrad. Stab.*, 2007, **92**, 480–489.
29 M. Jiang, Z. Zheng, X. Ding, X. Cheng and Y. Peng, *Colloid Polym. Sci.*, 2007, **285**, 1049–1054.
30 Y. Xu, L. Wang, Y. Tong, S. Xiang, X. Guo, J. Li, H. Gao and X. Wu, *J. Appl. Polym. Sci.*, 2016, **133**, 43844.
31 P. G. Shukla, B. Kalidhass, A. Shah and D. V. Palaskar, *J. Microencapsulation*, 2002, **19**, 293–304.
32 H. Zhang, H. Qin, L. Li, X. Zhou, W. Wang and C. Kan, *J. Agric. Food Chem.*, 2017, DOI: 10.1021/acs.jafc.7b01401.
33 J. Wang, Z. Zheng, Q. Wang, P. Du, J. Shi and X. Wang, *J. Appl. Polym. Sci.*, 2013, **128**, 4047–4057.
34 G. N. Antonow, *J. Chim. Phys.*, 1907, **5**, 372–385.
35 C. J. Vanoss, M. K. Chaudhury and R. J. Good, *Chem. Rev.*, 1988, **88**, 927–941.
36 M. C. Michalski, J. Hardy and B. J. V. Saramago, *J. Colloid Interface Sci.*, 1998, **208**, 319–328.
37 Z. Liu, R. Qie, W. Li, N. Hong, Y. Li, C. Li, R. Wang, Y. Shi, X. Guo and X. Jia, *New J. Chem.*, 2017, **41**, 3190–3195.
38 A. H. Al-Rohaimi, *J. Oleo Sci.*, 2015, **64**, 27–40.
39 K. Cui, D. Wang, H. Zhang, J. Guo, C. Cai, C. Zhu, N. Zhao and J. Xu, *J. Appl. Polym. Sci.*, 2017, **134**, 45280.
40 P. L. Ritger and N. A. Peppas, *J. Controlled Release*, 1987, **5**, 37–42.
41 X. Jia, W. B. Sheng, W. Li, Y. B. Tong, Z. Y. Liu and F. Zhou, *ACS Appl. Mater. Interfaces*, 2014, **6**, 19552–19558.
42 Z. Gu, X. Xu and L. Han, *Mod. Agrochem.*, 2003, **2**, 21–23.
43 P. Wagner, R. Fürstner, W. Barthlott and C. Neinhuis, *J. Exp. Bot.*, 2003, **54**, 1295–1303.